Theta-activity in anterior cingulate cortex predicts task rules and their adjustments following errors

Thilo Womelsdorf[a,1], Kevin Johnston[a], Martin Vinck[b], and Stefan Everling[a,c]

[a]Department of Physiology and Pharmacology, University of Western Ontario, London, ON N6A 5K8,Canada; [b]Cognitive and Systems Neuroscience Group, Center for Neuroscience, University of Amsterdam, 1098 XH Amsterdam, The Netherlands; and [c]Robarts Research Institute, London, ON N6A 5K8, Canada

Edited by Nancy J. Kopell, Boston University, Boston, MA, and approved January 26, 2010 (received for review June 4, 2009)

Accomplishing even simple tasks depend on neuronal circuits to configure how incoming sensory stimuli map onto responses. Controlling these stimulus-response (SR) mapping rules relies on a cognitive control network comprising the anterior cingulate cortex (ACC). Single neurons within the ACC convey information about currently relevant SR mapping rules and signal unexpected action outcomes, which can be used to optimize behavioral choices. However, its functional significance and the mechanistic means of interaction with other nodes of the cognitive control network remain elusive and poorly understood. Here, we report that core aspects of cognitive control are encoded by rhythmic theta-band activity within neuronal circuits in the ACC. Throughout task performance, theta-activity predicted which of two SR mapping rules will be established before processing visual target information. Task-selective theta-activity emerged particularly early during those trials, which required the adjustment of SR rules following an erroneous rule representation in the preceding trial. These findings demonstrate a functional correlation of cognitive control processes and oscillatory theta-band activity in macaque ACC. Moreover, we report that spike output of a subset of cells in ACC is synchronized to predictive theta-activity, suggesting that the theta-cycle could serve as a temporal reference for coordinating local task selective computations across a larger network of frontal areas and the hippocampus to optimize and adjust the processing routes of sensory and motor circuits to achieve efficient sensory-motor control.

cognitive control | theta-synchronization | attention | oscillation | antisaccade

Cognitive control refers to those neuronal processes responsible for assembling task-relevant information, which in turn biases sensory and motor pathways for efficient communication during task processing. Two core functions of cognitive control are (*i*) the implementation and maintenance of task-relevant stimulus-response (SR) mapping rules, and (*ii*) the adjustment and optimization of such representations during task performance according to behavioral outcome. Both functions are subserved by a mosaic of interconnected neuronal groups distributed within frontal cortex (1–4). The anterior cingulate cortex (ACC) is one of the key nodes within this cognitive control network, conveying task relevant information at various time intervals during task processing (5, 6). First, during preparatory periods, ACC neurons convey signals selective for the currently relevant SR mapping rule (7), and allow inferences with respect to changes in SR mapping triggered by either an incorrect response, or an explicit cue to change SR mapping (8). Second, during stimulus processing and delay epochs in working memory paradigms, subsets of neurons encode the expected reward outcome associated with the stimulus (9). Third, following the behavioral response to a target stimulus, neuronal groups in ACC signal whether the behavioral response was incorrect or resulted in unexpected reward outcome (10–13). Consequently, ACC neurons signal the adjustment of behavior following changes in task demands or unexpected outcomes on previous trials (8, 14, 15).

Taken together, these findings show that neuronal activity in ACC reflects major functions underlying successful cognitive control. However, the question of exactly how these diverse functions arise in neuronal spiking responses within the ACC and how they are communicated dynamically during task processing to other nodes of the cognitive control network remains unresolved.

One fundamental mechanism to achieve efficient and temporally dynamic neuronal communication of local computations within the ACC and between other nodes of the control network could be the synchronization of neuronal activity to common rhythmic fluctuations of neuronal excitability (16–20). According to this hypothesis, neuronal groups within the ACC are expected to synchronize dynamically during different task epochs. Moreover, the strength of oscillatory activity and of phase coherent spiking responses in ACC should convey task selective information. Despite these potentially fundamental consequences of rhythmic neuronal activity, there is only limited evidence for task selective and functionally relevant synchronization from within the ACC (21, 22).

However, neuronal circuitry in ACC gives rise to prominent theta-oscillations (23–25), which is believed to originate in an interneuron network in superficial layers (25, 26). theta-Oscillations are an ideal candidate to structure neuronal communication for a variety of reasons. First, many neurons spike preferentially at particular phases of the theta-cycle (27–31). Second, theta-oscillations are capable of shaping local high frequency γ-band synchronization, which is frequently nested within the theta-cycle (32–34) and indexes stimulus selection (35–37). Third, neuronal spiking output is synchronized to theta-activity ubiquitously in the brain, including the hippocampal formation, frontal cortex, and sensory cortices, and is therefore capable of providing a temporal context for coherent interareal communication (19, 34, 38, 39). Fourth, in humans, theta-activity in frontal cortex and hippocampus has been shown to increase with cognitive control demands and successful task performance. In particular, theta-activity increases with working memory load (40–43), and during visual search of targets in space (44), predicts successful encoding of visual and verbal stimuli in long-term memory (45–49) and indexes incorrect responses (50–52).

These multiple facets of theta-activity suggest that it could serve as a fundamental mechanism that allows neuronal groups in ACC to integrate and convey task-selective information. We therefore investigated the dynamic evolution of rhythmic activity in macaque ACC during a task-shift paradigm. The task required monkeys to respond to a peripheral stimulus according to two SR mapping rules, which changed without overt cue during the course of the task (Fig. S1*A*). We found that theta-frequency activity is the most prominent oscillatory signature during the preparatory task epoch.

Author contributions: K.J. and S.E. designed research; T.W., K.J., and S.E. performed research; T.W. and M.V. contributed new reagents/analytic tools; T.W. analyzed data; and T.W. and S.E. wrote the paper.

The authors declare no conflict of interest.

This article is a PNAS Direct Submission.

Freely available online through the PNAS open access option.

[1]To whom correspondence should be addressed. E-mail: thiwom@imaging.robarts.ca.

This article contains supporting information online at www.pnas.org/cgi/content/full/0906194107/DCSupplemental.

For one fourth of the recorded neuronal groups, theta-activity increased selectively for either of the two SR mapping rules and is stronger for correct versus incorrect trials. In addition, we found that theta-activity became task-selective earlier in time when cognitive control demands were high. Moreover, we show that rhythmic LFP theta-activity has consequences for spike output, with one third of all neurons synchronizing significantly to the theta-cycle during the preparatory period.

Results

Behavioral Adjustment Following Task Switches. We recorded in 39 sessions the local field potential (LFP) from one to five neuronal groups (28 and 11 in two monkeys, respectively). Monkeys performed, on average, 74.9% (78.1%) correct on the antisaccade (i.e., prosaccade) task, with lower accuracy in trials immediately following the task change (Fig. S1*B*; see ref. 7). Quantifying correct performance for successive sets of five trials with correct responses following the rule change revealed that accuracy asymptotes within 10 trials (Fig. S1*B*). In contrast to accuracy, saccadic reaction times remained constant with pro- and antisaccade latencies averaging to 199 and 228 ms, respectively (Fig. S1*B*). These behavioral results show that the behavioral adjustment required by the change in SR rule primarily affected preparatory processes required to instantiate and maintain a new SR rule, rather than a readjustment of movement parameters, which would be expressed as variations in saccade latency.

Task Selectivity of Theta-Activity. Applying the correct SR mapping rule at the time the target stimulus is presented requires advance preparation of neuronal circuitry to selectively represent the relevant task rule. We therefore calculated the evolution of oscillatory activity during the preparatory period from 3 to 30 Hz and quantified task selectivity for each neuronal site. Fig. S1*C* shows the average evolution of LFP power for an example site for the pro- and antisaccade task (Fig. S1*C Upper* and *Lower*, respectively), illustrating prominent theta-frequency activity, which decreases in strength on prosaccade trials and increases during antisaccade trials. We quantified this difference by calculating a task selectivity index (TSI) for each time-frequency data point and derived a statistical map with a cluster randomization approach correcting for multiple comparisons (*Materials and Methods*). For the example shown in Fig. S1*C*, task selectivity was significant for a 5- to 10-Hz theta-frequency band well in advance of peripheral stimulus presentation. The peak TSI value of 0.3 corresponds to 85.7% stronger LFP theta-power during the antisaccade task.

Across all sites, the emergence of task selectivity in the theta-band was the most prominent preparatory signature (Fig. 1*A*), predicting which SR rule was established before the onset of the stimulus. Across all 67 LFP sites, 23.8% (16) showed significant task selectivity during the preparatory time-frequency window in the theta-band, with 13.4% (10.4%) of sites showing enhanced theta-power when preparing the SR rule for the prosaccade (antisaccade) task. The proportion of task selectivity for either task was statistically not different (binomial test, $P > 0.05$). Sites selective for the anti- and prosaccade task overlapped spatially with a slight trend for antisaccade selective tasks to be more likely more anterior in area 24c. Selecting only those sites with a significant effect in the time-frequency window with the most prevalent task effects (5–10 Hz during the −0.4 to 0 s before stimulus onset) illustrates that task selectivity emerged at approximately −0.4 s before stimulus onset (Fig. 1*B*), and showed similar time-frequency dynamics for sites preferring pro- and antisaccades (Fig. 1*C*). This finding also illustrates that task selectivity of preparatory theta-activity is not confounded by a difference of the two tasks in terms of task difficulty.

Frequency Specific Trial-by-Trial Prediction of Task Rules. To analyze whether frequency-specific oscillatory activity can actually be used

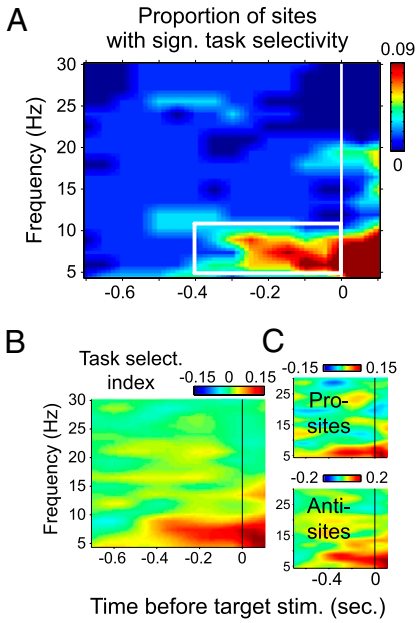

Fig. 1. Task selectivity of LFP power. (*A*), Proportion of sites with individually statistically significant task selectivity for the pro- or antisaccade task based on a cluster-based randomization test with multiple comparison correction. The statistical map reveals that task selectivity emerges in a narrow theta-frequency band (5–10 Hz) before target stimulus onset. The white box indicates the time-frequency region of interest used for later analysis. (*B*) Average task selectivity in the preparatory period for sites showing significant task selective theta-activity. (*C*) Average task selectivity plotted separately for sites preferring the prosaccade task (*Upper*) and the antisaccade task (*Lower*).

by neuronal circuitry to predict the forthcoming interpretation of a stimulus similar to firing rates (see ref. 7), we conducted a receiver operating characteristic (ROC) analysis. Fig. 2*A* illustrates that an ideal observer could predict which SR mapping will be applied before the stimulus appeared only when relying on theta-activity (5–10 Hz; one-sample *t* test, $P < 0.05$), but not when considering lower (2–4 Hz) or higher frequency bands in the low and high β-range (11.5–15.5 Hz and 18.5–22.5 Hz). The average ROC value began to be statistically significantly different from chance (ROC value of 0.5) already at −0.4 s before stimulus onset (one-sample *t* test, $P < 0.05$), with no other frequency band reaching statistical significance before stimulus onset (all $P > 0.05$; see Fig. 2*B*). Note that spike rates in ACC showed likewise the earliest significant ROC prediction at −0.4 s, but only in those trials immediately following the task rule change. In later trials, ACC spike rates distinguished both tasks at successively later times before stimulus onset (see ref. 7). We therefore analyzed the latency of task selectivity for successive subsets of five correct trials relative to the task rule change by measuring the time when the ROC prediction became significant ($P < 0.05$) for two successive time windows. Fig. 2*C* shows that task selectivity of LFP theta-activity remained rather constant across trials, emerging at −0.35 s in trials early after the task rule change, and at −0.4 s thereafter. No other frequency range than theta showed significant task selectivity before stimulus onset in any of the trial subsets. Likewise, the overall strength of the TSI in the −0.4 to 0 s time window before stimulus onset did not decrease after the initial task rule change (Fig. 2*D*). These findings contrast to the change in firing rate latencies reported in ACC before (7), illustrating that rate effects and LFP theta reflect different signals. Interestingly, significant task selectivity is available in spike rates at −0.4 s even after the fifth trial in the same task, not in ACC, but in other nodes of the cognitive control network (lateral PFC; see ref. 7). Thus, the early emerging task selectivity of LFP theta-activity in the ACC may well reflect information

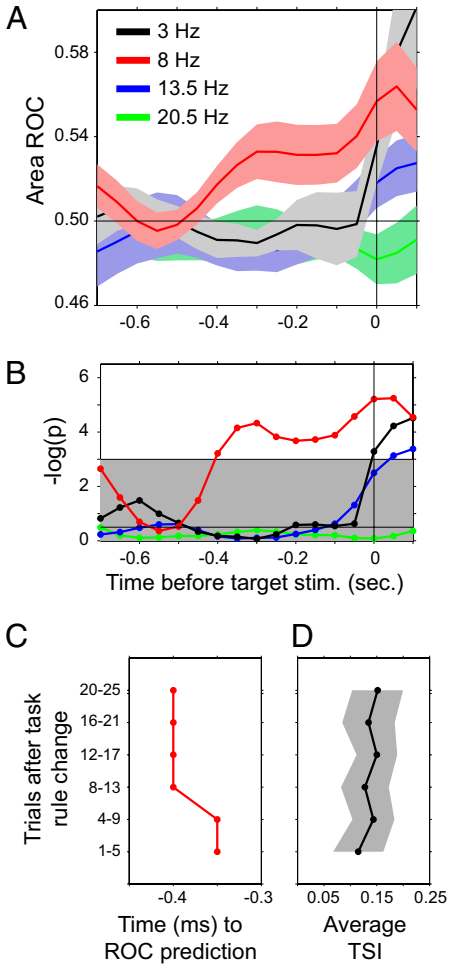

Fig. 2. Trial-by-trial (i.e., ROC) task prediction for power at different frequency bands, and its latency for trials relative to the change in task rule. (*A*) ROC values for successive time bins during the preparatory period. Shaded areas denote SEM. (*B*) *P* value evolution for the ROC values in *A*. Gray area shows the ≤2.998 = −log(0.05) region where trial-by-trial prediction of the task is not significant. Colors denote different frequency bands as indicated in *A*. (*C*) Latency of significant ROC prediction based on theta-power for trial sets relative to the task rule change. (*D*) Average TSI of theta-power for trial sets relative to the task rule change. Shaded areas show SEM.

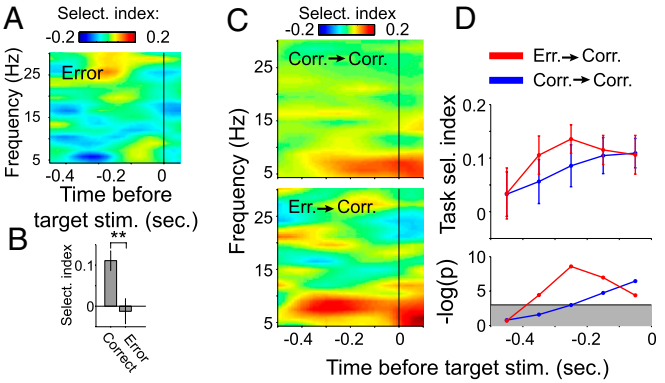

Fig. 3. Behavioral correlates of theta-frequency modulation for task-selective sites. (*A*) Average time-frequency distribution of the TSI for error trials (plotted in a color range similar to the TSI on correct trial shown in Fig. 1*B*). (*B*) Average (±SEM) TSI for correct and error trials for theta-power (5–10 Hz) in the −0.4 to 0 s before stimulus onset. Two stars denote statistical significant difference at $P < 0.01$. (*C*) Average TSI for correct trials following other correct trials (*Upper*) and for correct trials following errors (*Lower*). (*D*) (*Upper*) Average TSI of theta-power on correct trials following previous correct (*blue*) or error (*red*) trials calculated for successive time windows before stimulus onset. (*Bottom*) Statistical inference of TSIs, with significant values above gray shaded area.

available from input of other nodes of the cognitive control network, but without being necessarily translated into modulated overall spike counts (as described further later).

Theta-Activity and Behavioral Adjustment. The previous result leaves open whether the observed task-selective theta-activity reflects a genuine functional contribution from ACC with respect to cognitive control or is primarily inherited from other nodes of the network. In a first analysis addressing this issue, we compared task-selective theta-activity in correct trials and error trials, finding that task selective theta-activity was absent on error trials, in which the incorrect SR mapping rule had been applied to the peripheral stimulus (paired *t* test, $P < 0.01$; Fig. 3 *A* and *B*; note that we excluded from analysis the first trial after the task switch, which was per definition incorrect, but not indicative of a failure to maintain a SR rule). In a second analysis we tested, whether task-selective theta-activity in ACC reflects the adjustment of task rule representations following erroneous SR mapping. Previous results suggest that spike rates in ACC signal the behavioral outcome of a trial and provide the critical information to overcome erroneous representations well before other areas of the cognitive control network (5, 7, 15). We therefore analyzed task-selective theta-activity in correct trials that followed a previous error trial (i.e., *E-C*) with correct trials following other correct trials (i.e., *C-C*). Fig. 3*C* shows that task-selective theta-activity in *E-C* trials is similar in strength, but emerges earlier compared with *C-C* trials. To quantify this latency difference, we calculated the average TSI of theta-activity (5–10 Hz) within successive 0.1-s windows during the preparatory period. Fig. 3*D* reveals that task selectivity rose earlier in *E-C* trials, becoming statistically significant already within −0.4 to −0.3 s before stimulus onset (one-sample *t* test, $P < 0.05$). In contrast, task selectivity in *C-C* trials became significant later starting between −0.2 to −0.1 s before stimulus onset (Fig. 3*D*).

Consequences of Task-Selective Theta-Activity for Spike Output. To this point, task selectivity in the ACC was shown to emerge in a time- and frequency-selective LFP theta-band. It emerged early (at approximately −0.4 s before stimulus onset) even after the fifth trial following the task switch, i.e., where spike counts in ACC do not distinguish anymore between the tasks. These findings suggest that enhanced LFP theta-activity is functionally relevant, but rather than being translated into a higher spike count, it may provide a critical reference to structure spike output in time (29). To test this hypothesis, we analyzed for a subset of 22 most isolated single ACC neurons whether their spike output is phase locked (i.e., phase consistent) to LFP theta-activity and whether spike–LFP phase consistency increases during periods of enhanced LFP theta-activity. The analysis of spike–LFP phase consistency is nontrivial for neurons firing only few spikes (few samples) because common phase locking measures are biased toward higher values the smaller the sample size, rendering the phase locking statistics less reliable and imposing a serious confound when comparing conditions (here, tasks) with different sample sizes. However, even for neurons firing only sparsely in ACC, we observed that spikes often occur at particular phases of the theta-cycle. For illustration, Fig. 4*A* shows example traces of spikes of one sparsely firing neuron and the LFP (5–10 Hz passband) during three pro- and antisaccade trials. This example neuron is selected because it visualizes (i) that theta-power just before stimulus onset is stronger in only one (antisaccade) task, (ii) that spikes tend to occur around the time of the

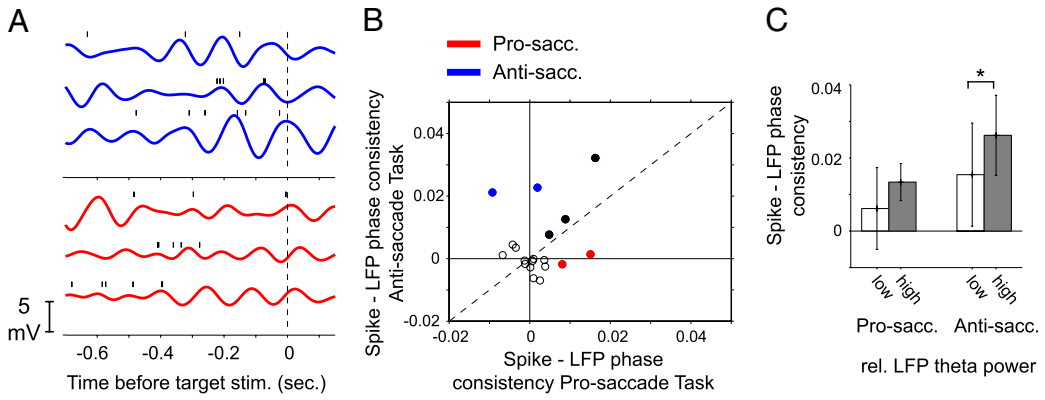

Fig. 4. Spike–LFP phase consistency in the theta-band can be task-selective and is stronger when theta-activity is larger. (*A*) Six example trials of a sparsely firing ACC neuron and the LFP (passband 5–10 Hz) during the preparatory period during pro- (*red*) and antisaccade (*blue*) trials. (*B*) Scatterplot of spike–LFP phase consistency for pro- (*x* axis) and antisaccade (*y* axis) trials. Filled circles show spike–LFP pairs with Rayleigh significant ($P < 0.05$) phase consistency for only the antisaccade task (*blue*), the prosaccade task (*red*), or both tasks (*black*). (*C*) Spike–LFP phase consistency for median split subsets of trials according to theta-power for either task separately, showing that, for the antisaccade task, spikes are on average significantly ($P < 0.05$) more synchronized to LFP theta when theta-power is stronger.

theta-cycle peak, rather than independent of the theta-cycle, and (iii) that this phase specificity becomes evident in the last 0.4 s before stimulus onset only for the antisaccade trials and not for the prosaccade trials. Measuring spike–LFP phase consistency across the whole sample of neurons for spikes within the 0.4-s window before stimulus onset showed that the spiking output of 31.8% of the neurons (7 of 22) were significantly phase-consistent to the LFP (Fig. 4*B*; Rayleigh test for circular homogeneity, $P < 0.05$). Among the phase-consistent neurons, three were significantly phase-locked in both tasks, but for four neurons spike–LFP phase consistency was task-selective (Fig. 4*B*). Critically, phase consistency tended to be stronger when LFP theta-activity was stronger (Fig. 4*C*). To test this, we median split for each neuron ($n = 22$) the theta-power distributions of the −0.4 to 0 s preparatory period from each task and calculated spike–LFP phase consistency separately for the subsets with high and low theta-activity and found that spike–LFP phase consistency was significantly stronger for the antisaccade task when theta-activity was stronger ($P < 0.05$, paired *t* test; Fig. 4*C*). For the prosaccade task the same pattern was observed, but the effect remained nonsignificant ($P = 0.3$, paired *t* test). Thus, there is overall evidence that the reported findings pertaining to task-selective LFP theta-activity have consequences for spiking output within ACC.

Discussion

Our results reveal that LFP theta-activity in ACC reflects core functions of a cognitive control network. We found that one quarter of all recorded neuronal groups selectively represented one of two task rules and maintained task-specific theta-activity throughout task performance. An ROC analysis showed that the forthcoming interpretation of a stimulus can be predicted already from 0.35 to 0.4 s before the stimulus appears. Predictive, task selective theta-activity was likely functionally relevant as it ceased on error trials, and emerged particularly early in time when an erroneous task representation in one trial was adjusted to the correct SR mapping rule in the trial following an error. In addition, we show that LFP theta-activity has consequences for spike output: For a subset of isolated single neurons, spiking responses phase-locked to the theta-cycle, an effect that tended to increase with increasing LFP theta-power and showed task selectivity similar to task selectivity of the LFP theta-activity. These results critically extend existing hypotheses regarding the role of ACC in cognitive control and suggest a mechanism for selective neuronal communication of task relevant information.

Previous models suggest that the specific role of the ACC in a larger cognitive control network lies in "monitoring of task performance" and evaluating "action outcome," informing other nodes of the network when task demands have varied over time or are particularly high (53, 54). In particular, these studies showed that the ACC is modulated in conditions of high task difficulty or conflict (e.g., in incongruent mapping conditions), when SR rules are changed implicitly, following altered reward contingencies (7, 8, 14, 15), or when previous trials were performed incorrectly (5, 55). Our results complement these findings by showing that neuronal groups in ACC signal the adjustment of SR rules following errors. Our findings show that this corrective signal was evident in the LFP being selective in time as early as 0.4 s before target stimulus processing, and selective in frequency, occurring in the theta-frequency band. Acknowledging that oscillatory theta-activity has been found ubiquitously within and between many brain areas during various cognitive processes suggest that it could reflect a mechanism underlying the coordination of neuronal interactions within a larger network pertaining to cognitive control (19, 56, 57).

This suggestion is also consistent with the finding that LFP theta-activity remained predictive of the correct task rule throughout all trials during a block of trials, emerging between 0.4 and 0.35 s before the visual target stimulus was presented. Interestingly, in our previous report on spike output in ACC and lateral prefrontal cortex using the same task design, we found that the earliest task selective signals emerged likewise at 0.4 s before stimulus onset, showing that task rule information becomes available at the same time in the larger cognitive control network. However, the latencies of task-predictive spike rate modulation differed between areas. In ACC spike rates were predictive at −0.4 s only during the first trials after the implicit task switch, and then gradually occurred later relative to stimulus onset at 0.25 and 0.05 s as more trials were performed on the same task in a block. The reverse pattern was found in lateral prefrontal cortex with spike output becoming significantly predictive at −0.4 s before stimulus onset only after the fifth trials following the task switch. These findings could reflect that task-selective LFP theta-activity in the ACC beginning at 0.4 s early and later after the task switch is partly inherited from other input areas of the control network, like the lateral prefrontal cortex, but without being translated into enhanced spike counts at the same early time period within ACC. This suggestion is consistent with the likely origin of the LFP, which is influenced by subthreshold, synaptic inputs from more distant areas, reflecting to its largest part a weighted sum of dendrosomatic synaptic signals and slower voltage-dependent membrane oscillations within a local patch of neuronal tissue (58).

Alternatively, instead of affecting the overall spike counts, LFP theta-activity in the ACC could rather modulate the timing

of spike output of neurons as is typically found in other areas (19). Corresponding to this suggestion, we found, even within a small sample of sparsely firing neurons, that spiking output of approximately 30% of cells were significantly structured by the theta-cycle, occurring preferably at particular phases of the underlying oscillation. Moreover, we found that spike–LFP phase consistency was task-selective in a subset of neurons, and tended to be stronger when theta-activity was stronger. These findings suggest that, for a larger neuronal group in ACC, a task-selective theta-rhythm is critically focusing spike output to a narrow time window within a theta-cycle of approximately 8 Hz (0.125 s). As a consequence, postsynaptic neuronal groups would receive spatially and temporally dense excitation, triggering a new chain of task-selective spiking output and potentially allowing to synchronize distant nodes of larger cognitive control network to a common underlying theta-rhythm. Although this scenario awaits to be tested directly, previous studies suggest that selective synchronization at theta- and/or higher γ-band frequencies among neuronal groups is indeed used by the brain to integrate and rapidly distribute task-relevant information (59, 60).

One interesting speculation relates the observed LFP theta-activity in the ACC to theta- activity recorded from the frontal midline in human EEG/MEG studies. Source localization analysis has frequently located its origin near or within the ACC (41, 51, 61–64), although it may likewise be influenced by bilateral prefrontal or subcortical sources (see ref. 21). Human frontal midline theta is known to be strongest following error responses and phase-locked to the response itself (12, 50, 51), but frontal midline theta-oscillations have been documented in attention and working memory paradigms, increasing with increased memory load (40, 41, 43). The theta-activity we observe resonates well with these studies, suggesting a close similarity in underlying neuronal circuits giving rise to theta- activity in monkeys and humans and lending strong support for human EEG/MEG approaches to study the time–frequency dynamics of cognitive control functions (52, 65).

In summary, our results provide insight into the selectivity of neuronal theta-band synchronization during the dynamic evolution of cognitive control of SR mapping rules. These findings suggest that theta-band oscillations, most likely emerging in superficial layers of the ACC, could be pivotal for the functional communication of selective control information within the mosaic of areas subserving efficient cognitive control.

Materials and Methods

Experimental Procedures and Paradigm. We collected data in two macaque monkeys following guidelines of the Canadian Council of Animal Care policy on the use of laboratory animals and the University of Western Ontario Council on Animal Care. Extracellular recordings commenced through a recording chamber with one to five tungsten electrodes on a daily basis, guided by an anatomical MR image to ensure targeting the ACC (area 24c; for details see ref. 7). Data acquisition and filtering were done with a multi-channel processor (Plexon), using a headstage with unit gain. The LFP was extracted with a passband filter (0.7–170 Hz), further amplified and digitized at 1 kHz. The powerline artifact was removed from 10-s-long data segments using a discrete Fourier transform filter as described before (36). Behavioral control and stimulus generation were accomplished with the cortex software package, monitoring eye position at 1 kHz with a scleral search coil (David Northmore). Each trial began with a centrally presented, white fixation spot, which was fixated for a variable period of 1.1 to 1.4 s Upon its offset, a peripheral white stimulus appeared (8° to the right or left with equal probability), signaling to the monkey to saccade within 500 ms either toward (i.e., prosaccade) or away from it to the mirror location (i.e., antisaccade) to receive a juice reward. The SR mapping rule (pro- vs. antisaccade) changed every 30 correct trials without overt cue.

Data Analysis. Analysis was performed with custom Matlab code (Mathworks), using the fieldtrip toolbox (http://www.ru.nl/fcdonders/fieldtrip/). We limited all analysis to the preparatory period from −0.75 to 0.15 s around the peripheral stimulus onset excluding stimulus-onset locked and saccade-related potentials occurring later in the trial. Time-resolved oscillatory activity was calculated, after subtracting the stimulus locked average potential, as LFP power from 3 to 30 Hz based on Hanning tapered Fourier transforms in ±0.334 s time windows calculated every 0.05 s (see ref. 36). To calculate statistical differences between task conditions, we applied a nonparametric cluster-based randomization approach based on the TSI as our test statistics and corrected for multiple comparison as described and validated before (see ref. 66). The TSI is calculated as [(pref task − None-pref task)/(pref task + none-pref task)], resulting in values of ±1 with positive values revealing stronger power for the preferred task. We calculated spike–LFP phases based on the Hanning tapered Fourier transforms of the LFP around ±0.334 of each spike. To measure phase consistency we calculated the average pairwise phase difference between spike-LFP phases, resulting in a completely bias-free measure of phase consistency, which is linearly related to the more commonly used phase locking value. The normalized pairwise phase consistency takes on values between 0 (random phase distribution) and 1 (complete consistency). For details, see ref. 67 and *SI Materials and Methods*.

ACKNOWLEDGMENTS. This research was supported by grants from the Canadian Institutes of Health Research.

1. Badre D, Hoffman J, Cooney JW, D'Esposito M (2009) Hierarchical cognitive control deficits following damage to the human frontal lobe. *Nat Neurosci* 12:515–522.
2. Dosenbach NU, Fair DA, Cohen AL, Schlaggar BL, Petersen SE (2008) A dual-networks architecture of top-down control. *Trends Cogn Sci* 12:99–105.
3. Dosenbach NU, et al. (2007) Distinct brain networks for adaptive and stable task control in humans. *Proc Natl Acad Sci USA* 104:11073–11078.
4. Lee D, Rushworth MF, Walton ME, Watanabe M, Sakagami M (2007) Functional specialization of the primate frontal cortex during decision making. *J Neurosci* 27: 8170–8173.
5. Mansouri FA, Tanaka K, Buckley MJ (2009) Conflict-induced behavioural adjustment: a clue to the executive functions of the prefrontal cortex. *Nat Rev Neurosci* 10: 141–152.
6. Paus T (2001) Primate anterior cingulate cortex: where motor control, drive and cognition interface. *Nat Rev Neurosci* 2:417–424.
7. Johnston K, Levin HM, Koval MJ, Everling S (2007) Top-down control-signal dynamics in anterior cingulate and prefrontal cortex neurons following task switching. *Neuron* 53:453–462.
8. Williams ZM, Bush G, Rauch SL, Cosgrove GR, Eskandar EN (2004) Human anterior cingulate neurons and the integration of monetary reward with motor responses. *Nat Neurosci* 7:1370–1375.
9. Kennerley SW, Dahmubed AF, Lara AH, Wallis JD (2008) Neurons in the frontal lobe encode the value of multiple decision variables. *J Cogn Neurosci* 21:1162–1178.
10. Ito S, Stuphorn V, Brown JW, Schall JD (2003) Performance monitoring by the anterior cingulate cortex during saccade countermanding. *Science* 302:120–122.
11. Amiez C, Joseph JP, Procyk E (2005) Anterior cingulate error-related activity is modulated by predicted reward. *Eur J Neurosci* 21:3447–3452.
12. Luu P, Tucker DM, Makeig S (2004) Frontal midline theta and the error-related negativity: neurophysiological mechanisms of action regulation. *Clin Neurophysiol* 115:1821–1835.
13. Seo H, Lee D (2007) Temporal filtering of reward signals in the dorsal anterior cingulate cortex during a mixed-strategy game. *J Neurosci* 27:8366–8377.
14. Shima K, Tanji J (1998) Role for cingulate motor area cells in voluntary movement selection based on reward. *Science* 282:1335–1338.
15. Kennerley SW, Walton ME, Behrens TE, Buckley MJ, Rushworth MF (2006) Optimal decision making and the anterior cingulate cortex. *Nat Neurosci* 9:940–947.
16. Womelsdorf T, Fries P (2009) Selective attention through selective synchronizaiton. *The Cognitive Neurosciences*, ed Gazzaniga M (MIT Press, Cambridge, MA), Vol 4.
17. Schroeder CE, Lakatos P (2009) Low-frequency neuronal oscillations as instruments of sensory selection. *Trends Neurosci* 32:9–18.
18. Sejnowski TJ, Paulsen O (2006) Network oscillations: emerging computational principles. *J Neurosci* 26:1673–1676.
19. Buzsaki G (2006) *Rhythms of the Brain* (Oxford University Press Inc., Oxford, New York).
20. Haider B, McCormick DA (2009) Rapid neocortical dynamics: cellular and network mechanisms. *Neuron* 62:171–189.
21. Mitchell DJ, McNaughton N, Flanagan D, Kirk IJ (2008) Frontal-midline theta from the perspective of hippocampal "theta". *Prog Neurobiol* 86:156–185.
22. Tsujimoto T, Shimazu H, Isomura Y (2006) Direct recording of theta oscillations in primate prefrontal and anterior cingulate cortices. *J Neurophysiol* 95:2987–3000.
23. Colom LV, Christie BR, Bland BH (1988) Cingulate cell discharge patterns related to hippocampal EEG and their modulation by muscarinic and nicotinic agents. *Brain Res* 460:329–338.
24. Talk A, Kang E, Gabriel M (2004) Independent generation of theta rhythm in the hippocampus and posterior cingulate cortex. *Brain Res* 1015:15–24.
25. Wang C, Ulbert I, Schomer DL, Marinkovic K, Halgren E (2005) Responses of human anterior cingulate cortex microdomains to error detection, conflict monitoring, stimulus-response mapping, familiarity, and orienting. *J Neurosci* 25:604–613.
26. Hedberg TG, Simpson GV, Stanton PK (1993) Microcircuitry of posterior cingulate cortex in vitro: electrophysiology and laminar analysis using the current source density method. *Brain Res* 632:239–248.

27. Klausberger T, Somogyi P (2008) Neuronal diversity and temporal dynamics: the unity of hippocampal circuit operations. *Science* 321:53–57.
28. Volgushev M, Chistiakova M, Singer W (1998) Modification of discharge patterns of neocortical neurons by induced oscillations of the membrane potential. *Neuroscience* 83:15–25.
29. Kamondi A, Acsády L, Wang XJ, Buzsáki G (1998) Theta oscillations in somata and dendrites of hippocampal pyramidal cells in vivo: activity-dependent phase-precession of action potentials. *Hippocampus* 8:244–261.
30. Montgomery SM, Sirota A, Buzsáki G (2008) Theta and gamma coordination of hippocampal networks during waking and rapid eye movement sleep. *J Neurosci* 28: 6731–6741.
31. Jacobs J, Kahana MJ, Ekstrom AD, Fried I (2007) Brain oscillations control timing of single-neuron activity in humans. *J Neurosci* 27:3839–3844.
32. Canolty RT, et al. (2006) High gamma power is phase-locked to theta oscillations in human neocortex. *Science* 313:1626–1628.
33. Csicsvari J, Jamieson B, Wise KD, Buzsáki G (2003) Mechanisms of gamma oscillations in the hippocampus of the behaving rat. *Neuron* 37:311–322.
34. Sirota A, et al. (2008) Entrainment of neocortical neurons and gamma oscillations by the hippocampal theta rhythm. *Neuron* 60:683–697.
35. Fries P (2009) Neuronal gamma-band synchronization as a fundamental process in cortical computation. *Annu Rev Neurosci* 32:209–224.
36. Womelsdorf T, Fries P (2007) The role of neuronal synchronization in selective attention. *Curr Opin Neurobiol* 17:154–160.
37. Womelsdorf T, Fries P, Mitra PP, Desimone R (2006) Gamma-band synchronization in visual cortex predicts speed of change detection. *Nature* 439:733–736.
38. Kahana MJ (2006) The cognitive correlates of human brain oscillations. *J Neurosci* 26: 1669–1672.
39. Raghavachari S, et al. (2001) Gating of human theta oscillations by a working memory task. *J Neurosci* 21:3175–3183.
40. Jensen O, Tesche CD (2002) Frontal theta activity in humans increases with memory load in a working memory task. *Eur J Neurosci* 15:1395–1399.
41. Gevins A, Smith ME, McEvoy L, Yu D (1997) High-resolution EEG mapping of cortical activation related to working memory: effects of task difficulty, type of processing, and practice. *Cereb Cortex* 7:374–385.
42. Deiber MP, et al. (2007) Distinction between perceptual and attentional processing in working memory tasks: a study of phase-locked and induced oscillatory brain dynamics. *J Cogn Neurosci* 19:158–172.
43. Scheeringa R, et al. (2009) Trial-by-trial coupling between EEG and BOLD identifies networks related to alpha and theta EEG power increases during working memory maintenance. *Neuroimage* 44:1224–1238.
44. Ekstrom AD, et al. (2005) Human hippocampal theta activity during virtual navigation. *Hippocampus* 15:881–889.
45. Osipova D, et al. (2006) Theta and gamma oscillations predict encoding and retrieval of declarative memory. *J Neurosci* 26:7523–7531.
46. Sarnthein J, Petsche H, Rappelsberger P, Shaw GL, von Stein A (1998) Synchronization between prefrontal and posterior association cortex during human working memory. *Proc Natl Acad Sci USA* 95:7092–7096.
47. Sederberg PB, Kahana MJ, Howard MW, Donner EJ, Madsen JR (2003) Theta and gamma oscillations during encoding predict subsequent recall. *J Neurosci* 23: 10809–10814.
48. Rizzuto DS, et al. (2003) Reset of human neocortical oscillations during a working memory task. *Proc Natl Acad Sci USA* 100:7931–7936.
49. Mormann F, et al. (2005) Phase/amplitude reset and theta-gamma interaction in the human medial temporal lobe during a continuous word recognition memory task. *Hippocampus* 15:890–900.
50. Mazaheri A, Nieuwenhuis IL, van Dijk H, Jensen O (2009) Prestimulus alpha and mu activity predicts failure to inhibit motor responses. *Hum Brain Mapp* 30:1791–1800.
51. Debener S, et al. (2005) Trial-by-trial coupling of concurrent electroencephalogram and functional magnetic resonance imaging identifies the dynamics of performance monitoring. *J Neurosci* 25:11730–11737.
52. Fan J, et al. (2007) The relation of brain oscillations to attentional networks. *J Neurosci* 27:6197–6206.
53. Cohen JD, Botvinick M, Carter CS (2000) Anterior cingulate and prefrontal cortex: who's in control? *Nat Neurosci* 3:421–423.
54. Richmond BJ, Liu Z, Shidara M (2003) Neuroscience. Predicting future rewards. *Science* 301:179–180.
55. Kerns JG, et al. (2004) Anterior cingulate conflict monitoring and adjustments in control. *Science* 303:1023–1026.
56. Kirk IJ, Mackay JC (2003) The role of theta-range oscillations in synchronising and integrating activity in distributed mnemonic networks. *Cortex* 39:993–1008.
57. Fries P (2005) A mechanism for cognitive dynamics: neuronal communication through neuronal coherence. *Trends Cogn Sci* 9:474–480.
58. Logothetis NK (2003) The underpinnings of the BOLD functional magnetic resonance imaging signal. *J Neurosci* 23:3963–3971.
59. Gregoriou GG, Gotts SJ, Zhou H, Desimone R (2009) High-frequency, long-range coupling between prefrontal and visual cortex during attention. *Science* 324: 1207–1210.
60. Womelsdorf T, et al. (2007) Modulation of neuronal interactions through neuronal synchronization. *Science* 316:1609–1612.
61. Asada H, Fukuda Y, Tsunoda S, Yamaguchi M, Tonoike M (1999) Frontal midline theta rhythms reflect alternative activation of prefrontal cortex and anterior cingulate cortex in humans. *Neurosci Lett* 274:29–32.
62. Scheeringa R, et al. (2008) Frontal theta EEG activity correlates negatively with the default mode network in resting state. *Int J Psychophysiol* 67:242–251.
63. Pizzagalli DA, Oakes TR, Davidson RJ (2003) Coupling of theta activity and glucose metabolism in the human rostral anterior cingulate cortex: an EEG/PET study of normal and depressed subjects. *Psychophysiology* 40:939–949.
64. Miwakeichi F, et al. (2004) Decomposing EEG data into space-time-frequency components using Parallel Factor Analysis. *Neuroimage* 22:1035–1045.
65. Siegel M, Donner TH, Oostenveld R, Fries P, Engel AK (2008) Neuronal synchronization along the dorsal visual pathway reflects the focus of spatial attention. *Neuron* 60: 709–719.
66. Maris E, Oostenveld R (2007) Nonparametric statistical testing of EEG- and MEG-data. *J Neurosci Methods* 164:177–190.
67. Vinck M, van Wingerden M, Womelsdorf T, Fries P, Pennartz CM (2010) *Neuroimage*, 10.1016/j.neuroimage.2010.01.073.